Usability of 11C-methionine positron emission tomography for differentiation of intracranial brain tumor from non-neoplastic lesions before treatment

Tomohiro Yamaki (yamakitomohiro@hotmail.com)
Rehabilitation Center for Traumatic Apallics Chiba
Yoshinori Higuchi
Chiba University
Yasuo Iwadate
Chiba University
Tomoo Matsutani
Chiba University
Seiichiro Hirono
Chiba University
Hikaru Sasaki
Keio University
Sasao Ryota
Keio University
Masahiro Toda
Keio University
Shinji Onodera
Rehabilitation Center for Traumatic Apallics Chiba
Nobuo Oka
Rehabilitation Center for Traumatic Apallics Chiba
Shigeki Kobayashi
Rehabilitation Center for Traumatic Apallics Chiba

Research Article

Keywords: 11C-METPET, brain tumor, tomography

Posted Date: September 9th, 2021

DOI: https://doi.org/10.21203/rs.3.rs-871465/v1

Abstract

We investigated the usability of 11C-methionine positron emission tomography (11C-METPET) for the differentiation of intracranial brain tumors from non-neoplastic lesions before treatment. Among 425 consecutive patients who underwent 11C-METPET imaging, 113 pretreatment patients were analyzed. Quantitative data including mean, peak, and maximum standardized uptake values and the ratios of lesion uptake to mean and maximum contralateral normal frontal lobe gray matter uptake (Lmax/Nmean and Lmax/Nmax), were analyzed. Next, the optimal cut-off for the differential diagnosis of brain tumors from non-neoplastic lesions were determined using receiver-operating characteristics curves. Finally, positive and negative predictive value were calculated. The final diagnoses for brain tumors included central nervous system tumor, lymphoma, and metastatic brain tumor, whereas the non-neoplastic lesions included neurovascular disease, dysplasia, encephalopathy, and inflammatory disease. An Lmax/Nmax of greater than 2.01 and an Lmax/Nmean of greater than 2.23 provided the best sensitivity and specificity for the differential diagnosis of brain tumor. However, the positive and negative predictive value were 96.5% and 47.4%, respectively, for Lmax/Nmax, and 93.7% and 50%, respectively, for Lmax/Nmean. Considering high positive predictive value and low negative predictive value in relation to the diagnosis based on the optimal cut-off, the utilization of 11C-METPET imaging before treatment requires careful attention.

Introduction

Although, computed tomography (CT) and magnetic resonance imaging (MRI) are the main diagnostic imaging methods used for differentiation of intracranial lesions in initial medical examinations [1,2], these neuroimaging examinations do not always allow diagnosis of the correct pathological condition, and it is often difficult to plan the treatment strategy [3-5]. In the case of brain tumors in particular, the examinations for definitive diagnosis may be highly invasive, and the tumors require careful differentiation [6]. Recently, L-methyl-11C-methionine positron emission tomography (11C-METPET) has become relatively available and easy to use for further assessment and the provision of supportive information for deciding on the treatment strategy [7-9]. Methionine uptake is higher in tumor tissues than in normal tissues, and it shows good visual contrast [7]. Currently, 11C-METPET is often used for tumor grading, identification of the tumor margin in surgery or radiotherapy, discrimination between radiation necrosis and recurrence, prognosis prediction, and assessment of therapeutic effects [10-18]. However, there are few reports evaluating the usability of 11C-METPET when it is used as an initial diagnostic tool for pretreatment intracranial lesions. The objectives of this study were to evaluate the usability of 11C-METPET for the differentiation of brain tumors from non-neoplastic lesions.

Materials And Methods

Patients

Between April 2017 and August 2020, 425 consecutive patients with suspected brain tumors (206 men and 219 women; mean age 54.0 ± 17.0 years [± standard deviation; SD]) were referred from 33 hospitals and underwent a brain 11C-METPET scan. Among this group, 131 patients with a suspected brain tumor who had not been treated previously were examined to determine their primary differential diagnosis before treatment, and 294 patients were examined for secondary differentiation of recurrent tumors after treatment (Fig. 1). To verify the final diagnoses in the 131 pretreatment patients, the queries for the attending physicians who ordered the 11C-METPET imaging was performed. Overall, written responses were obtained for 113 patients (86.3%). The definitive diagnosis was determined by the doctor-in-charge of each hospital based on the longitudinal follow-up, including pathologic confirmation from resected or biopsied tumor, neuroimaging, and biochemical analysis. Finally, 101 patients (51 men and 50 women; mean age 51.4 ± 19.0 years [SD]) were confirmed with a definitive diagnosis. The pathologically confirmed brain tumors according to the World Health Organization 2016 classification included 31 high-grade central nervous system (CNS) tumors (glioblastoma, n=20; anaplastic astrocytoma, n=6; diffuse midline glioma, n=3; anaplastic oligodendroglioma, n=1; anaplastic oligodendroglioma or anaplastic oligoastrocytoma, n=1), 37 low-grade CNS tumors (oligodendroglioma, n=15; diffuse astrocytoma, n=10; pilocytic astrocytoma, n=3; ganglioglioma, n=2; dysembryoplastic neuroepithelial tumor, n=1; fibrillary astrocytoma, n=1; hemangioblastoma, n=1; liponeurocytoma, n=1; optic nerve glioma, n=1; subependymoma, n=1; tanycytic ependymoma, n=1), 5 otherwise unspecified glioma, 3 diffuse large B cell lymphoma, and 2 metastatic brain tumors (fallopian tube cancer, n=1; unknown origin, n=1). The non-neoplastic lesions included 10 cases of neurovascular disease (cerebral infarction, n=5; cerebral hemorrhage, n=4; moyamoya disease, n=1), 5 cases of dysplasia (cortical dysplasia, n=1; hippocampal sclerosis, n=1; hypothalamic hamartoma, n=1; normal subtype, n=2), 4 cases of encephalopathy (encephalopathy, n=3; posterior reversible encephalopathy syndrome, n=1), and 4 cases of inflammatory disease (acute disseminated encephalomyelitis, n=1; hypertrophic pachymeningitis, n=1; tumefactive multiple sclerosis, n=1; vasculitis, n=1; Fig. 2 and Table 2).

This study was approved by Rehabilitation Center for Traumatic Apallics Chiba review board and all subjects signed an informed consent form. The procedures used in this study adhere to the tenets of the Declaration of Helsinki. The clinical trial registration number is UMIN000042984 (www.umin.ac.jp/ctr/index/htm), which is retrospectively registered at 13 January, 2021.

11C-MET PETCT acquisition

11C-MET was first produced by the 14N(p, α) 11C nuclear reaction using a 16.5 MeV PETtrace cyclotron (GE Healthcare, Chicago, USA) according to previously reported methodology, and was prepared using the method of Ishiwata et al.[19, 20].

The mean administered mass radioactivity of 11C-MET was 371.2 ± 51.4 MBq (range 109.7–550.6 MBq; 10.0 ± 1.4 mCi; range 3.0–14.9 mCi). Before injection of 11C-MET, patients fasted for at least 6 hours. Patients then received an intravenous injection of 11C-MET according to the guidelines of the Japanese Society of Nuclear Medicine (http://jsnm.org/). After injection, the patients rested for approximately 10 minutes before image acquisition. Low-dose transmission CT images and PET images were obtained using GE scanners (Discovery MI® PETCT, GE Healthcare, Chicago, USA) and standard iterative reconstruction (192 × 192 matrix, 250 × 250-mm field of view, 1.3 x 1.3 x 2.79 mm voxel size) using a vendor-supplied algorithm. CT acquisition parameters included slice thickness of 3.75 mm, tube rotation of 0.8 s, table speed of 2.06 cm/rotation, pitch factor of 0.52 for helical CT, tube voltage of 120 kVp, and tube current of 150 mA with dose modulation. All 11C-METPET data were acquired in three-dimensional time-of-flight mode. The acquisition time per bed was 10 minutes. CT images and 11C METPET scans were coregistered using vendor-supplied software (AW Volume Share 7, GE Healthcare).

Image analysis

All PET scans acquired for pretreatment radiological diagnosis were interpreted by three medical personnel including a board-certified nuclear medicine physician, a board-certified neurosurgeon, and an experienced radiological technologist with medical records including CT and MRI. The regional methionine uptake was expressed as standardized uptake value (SUV). The area with the highest uptake in comparison with adjacent normal tissue was selected as the region of interest (ROI), avoiding any cystic or necrotic tissue. An ROI for each lesion was outlined according to the 50% of maximum uptake isocontour. If there was no abnormal uptake of 11C-MET on PET, the ROI was set according to the area of abnormal findings on MRI or CT. The mean SUV of the ROI pixels (SUVmean), the maximum SUV (SUVmax), and the maximum average SUV within a 1 cm^3 spherical volume (SUVpeak) were generated for the lesion ROI [21]. Lesion-to-normal tissue (L/N) ratios were measured by dividing the SUVmax of the lesion by the SUVmean of the contralateral normal frontal-lobe gray matter (Lmax/Nmean) and dividing the SUVmax of the lesion by the SUVmax of the contralateral normal frontal-lobe gray matter (Lmax/Nmax). In the case of bilateral lesions, the reference areas were selected in unaffected remote tissue.

Statistical analysis

All statistical analyses were performed using IBM SPSS Statistics 25.0 (IBM Corp., Armonk, NY, USA). Quantitative values are reported as arithmetic means ± SD. The values of SUVmean, SUVmax, SUVpeak, Lmax/Nmean, and Lmax/Nmax were compared separately using the Mann-Whitney nonparametric test. Receiver-operating-characteristics (ROC) curve analysis was used to determine the optimal index for 11C-MET PET. Cut-off values for key parameters were inferred according to Youden's index [22]. For all analyses, a p value of less than 0.05 was considered statistically significant.

Results

Of the 425 patients who underwent 11C-METPET, 101 patients had a definitive diagnosis for inclusion in this study. The demographics of this study population are summarized in Fig. 1.

Comparison of radiological diagnosis on 11C-METPET with final diagnosis

Comparisons between the radiological diagnoses on 11C-METPET and final diagnoses are summarized in Table 1. The concordance rates between radiological and definitive diagnoses were 88.6% for brain tumors and 67.9% for non-neoplastic lesions. The values of each 11C-METPET parameter, including SUVmean, SUVmax, SUVpeak, Lmax/Nmean, and Lmax/Nmax, are shown in Fig. 3 and Table 2. The measured parameter values were all significantly higher for the brain tumors than for the non-neoplastic lesions ($p < 0.001$).

ROC analysis of diagnostic accuracy for each 11C-METPET parameter

To determine optimal cut-off values for the differentiation of brain tumors from non-neoplastic lesions, receiver-operating-characteristics (ROC) and area under the curve (AUC) analyses were performed. The AUCs were 0.843 for Lmax/Nmean, 0.853 for Lmax/Nmax, 0.821 for SUVmax, 0.837 for SUVpeak, and 0.829 for SUVmean (Fig. 4). These data indicate that the L/N ratios showed better performance than the SUV parameters for differentiating between brain tumors and non-neoplastic lesions. Based on Youden's index, an Lmax/Nmax of 2.01 and Lmax/Nmean of 2.23 provided the best sensitivity and specificity for detection of brain tumors, with sensitivity and specificity of 70.5% and 91.3%, respectively, for Lmax/Nmax, and 75.6% and 82.6%, respectively, for Lmax/Nmean. In addition, the positive predictive value and negative predictive value were 96.5% and 47.4%, respectively, for Lmax/Nmax, and 93.7% and 50%, respectively, for Lmax/Nmean (Table 3).

Discussion

This study was undertaken to evaluate the usability of 11C-METPET for the differentiation between brain tumors and non-neoplastic lesions before treatment. Our data demonstrating the positive predictive value of 11C-METPET indicate that subjects with a positive screening test are truly likely to have a brain tumor, although a negative screening test because of low methionine uptake does not mean that subjects are free of brain tumor. In particular, low grade CNS tumor with a low level of methionine uptake is difficult to distinguish from non-neoplastic lesions. Herholz et al. found that the optimal L/N value cut-off for the discrimination of tumor from non-neoplastic lesions was 1.47, which provided a sensitivity of 76% and specificity of 87% [23]. However, our data showed an optimal cut-off of 2.01 for Lmax/Nmax and 2.23 for Lmax/Nmean. These higher values may be related to the wide range of pathology investigated in our study, which included various types of non-neoplastic lesions such as encephalopathy and lesions resulting from inflammatory diseases. However, it should be noted that the diagnostic accuracy of both the specialists and the optimal cut-off values for the low 11C-MET tracer uptake lesions were not high, indicating the limitations of using 11C-MET tracer uptake for diagnosis at the first visit. It was recently reported that it is easy to mistake non-neoplastic lesions for brain tumors on F-DOPAPET imaging [24]. It may be necessary to inform the attending physician planning the next strategy of the limitations of 11C-METPET.

11C-MET tracer uptake is dependent on the expression of L-type amino acid transporter [25]. Previous reports showed that it is useful for differentiating between recurrence and radiation necrosis in glioma and metastatic brain tumors after radiotherapy [10-18]. Although a brain tumor may show tumor proliferation, new collateral circulation, and pathological disruption of the blood brain barrier, diagnosis at the first visit is extremely important because the lesion may be in a place that is not easily accessible by surgery or is at high risk for intra or postoperative mortality [26, 27]. First-visit 11C-METPET results have recently been reported for various types of non-neoplastic lesions such as neurovascular disease, encephalopathy, and inflammatory disease [28-31]. However, it is difficult to identify non-neoplastic lesions by 11C-METPET parameters alone, including by the L/N ratio or the interpretation of nuclear medicine professionals. Therefore, we believe that more accurate radiological diagnosis will be obtained if an integrated shape recognition function using artificial intelligence is developed, in addition to using SUVs and L/N ratios as a method for distinguishing between brain tumors and non-tumor lesions [32-35].

This study has several limitations. First, this study is lack of pathological information in many of non-neoplastic lesions and a small number of patients with non-neoplastic lesions. In practice, it is difficult to obtain a pathological diagnosis of non-neoplastic lesions, therefore a longer observation period will be required in future study. Second, not all intracranial diseases were included in this study, such as tumors like infective or inflammatory granulomas. If the proportion of non-neoplastic lesions with inflammatory disease changes, the optimum cut-off value may also change [36, 37]. Furthermore, in case of neurovascular disease or inflammatory disease, methionine uptake rate must change depending on time interval from onset. Such information was not included from this study, which influenced the radiological image interpretation.

However, to the best of our knowledge, this study included the greatest number of first-visit intracranial disorders (including tumors and non-neoplastic lesions) yet included in an 11C-METPET study before treatment. In particular, there is much debate about the lesions with low methionine uptake. Further prospective studies using 11C-METPET before treatment are needed to evaluate the usability of 11C-METPET.

Conclusion

11C-METPET is often considered as an important tool for differentiating intracranial brain tumors from non-neoplastic lesions before treatment and planning the treatment strategy. However, the high positive predictive value and low negative predictive value in relation to the diagnosis of the optimal cut-off mean that the utilization of 11C-METPET needs for caution in patients before treatment. Further investigations are needed for the importance of the usability of 11C-METPET before treatment.

Declarations

Acknowledgements

We thank Dr. Masanori Itou and Dr. Hidehiro Okura at Juntendo University Urayasu Hospital; Dr Satoshi Inoue at Tokyo Dental College Ichikawa General Hospital; Dr. Toshihiko Iuchi, Dr. Yuzo Hasegawa, and Dr. Tsukasa Sakaida at Chiba Cancer Center; Dr. Ryuichi Kanai at Eiju General Hospital; Dr. Masato Nakaya at Keio University School of Medicine; Dr. Koichi Tamaki, Dr. Takeshi Fukushima, Dr. Minami Sasaki, and Dr. Ai Ishikawa at Matsudo City General Hospital; Dr. Tomihiro Wakamiya at International University of Health and Welfare Narita Hospital; Dr. Izumi Suda and Dr. Reiji Aoki at Narita Red Cross Hospital; Dr. Takao Fukushima at Takashimadaira Chuo General Hospital; Dr. Seiichiro Mine and Dr. Masaki Izumi at Chiba Cerebral and Cardiovascular Center; and Dr. Kentaro Horiguchi at Chiba University Graduate School of Medicine for cooperation with pathological and medical information. We also thank Karl Embleton, PhD, from Edanz Group (https://en-author-services.edanz.com/) for editing a draft of this manuscript.

Authors' contributions

All authors contributed to the study conception and design. Material preparation, data collection and analysis were performed by TY and YH. The first draft of the manuscript was written by TY and all authors commented on previous versions of the manuscript. All authors read and approved the final manuscript.

Competing interests

The authors state that they have no other potential conflicts of interest relevant to this study.

Data availability

The datasets analyzed during the current study are not publicly available due to the privacy are not public but are available from the corresponding author on reasonable request.

References

1. Masdeu, J.C., Gadhia, R., Faridar, A. Brain CT and MRI: differential diagnosis of imaging findings. *Handb. Clin. Neurol.* **136**, 1037-54 (2016).

2. Al-Okaili, R.N. *et al.* Intraaxial brain masses: MR imaging-based diagnostic strategy–initial experience. *Radiology.* **243**, 539-50 (2007).

3. Hardy, T.A. Pseudotumoral demyelinating lesions: diagnostic approach and long-term outcome. *Curr. Opin. Neurol.* **32**, 467-74 (2019).

4. Renard, D., Castelnovo, G., Le Floch, A., Guillamo, J.S., Thouvenot, E. Pseudotumoral brain lesions: MRI review. *Acta Neurol. Belg.* **117**, 17-26 (2017).

5. Law, L.Y., Riminton DS, Nguyen M, Barnett MH, Reddel SW, Hardy TA. The spectrum of immune-mediated and inflammatory lesions of the brainstem: clues to diagnosis. *Neurology.* **93**, 390-405 (2019).

6. Weller, M. *et al.* Glioma. *Nat. Rev. Dis. Primers.* **1**, 15017; 10.1038/nrdp.2015.17 (2015).

7. Glaudemans AW *et al.* Value of 11C-methionine PET in imaging brain tumours and metastases. *Eur. J. Nucl. Med. Mol. Imaging.* **40**, 615-635 (2013).

8. de Zwart, P.L. *et al.* Diagnostic accuracy of PET tracers for the differentiation of tumor progression from treatment-related changes in high-grade glioma: a systematic review and metaanalysis. *J. Nucl. Med.* **61**, 498-504 (2020).

9. Treglia, G. *et al.* Diagnostic performance and prognostic value of PET/CT with different tracers for brain tumors: a systematic review of published meta-analyses. *Int. J. Mol. Sci.* **20**, 4669; 10.3390/ijms20194669 (2019).

10. Falk Delgado, A., Falk Delgado, A. Discrimination between primary low-grade and high-grade glioma with 11 C-methionine PET: a bivariate diagnostic test accuracy meta-analysis. *Br. J. Radiol.* **1082**, 20170426; 10.1259/bjr.20170426 (2018).

11. Katsanos, A.H., Alexiou, G.A., Fotopoulos, A.D., Jabbour, P., Kyritsis, A.P., Sioka, C. Performance of 18F-FDG, 11C-methionine, and 18F-FET PET for glioma grading: a meta-analysis. *Clin. Nucl. Med.* **44**, 864-869 (2019).

12. Wang Y. *et al.* 11C methionine PET (MET-PET) Imaging of glioblastoma for detecting postoperative residual disease and response to chemoradiation therapy. *Int. J. Radiat. Oncol. Biol. Phys.* **102**, 1024-1028 (2018).

13. Takenaka, S. *et al.* Comparison of (11)C-methionine, (11)C-choline, and (18)F-fluorodeoxyglucose-PET for distinguishing glioma recurrence from radiation necrosis. *Neurol Med Chir (Tokyo).* **54**, 280-289 (2014).

14. Kits, A., Martin, H., Sanchez-Crespo, A., Delgado, A.F. Diagnostic accuracy of 11 C-methionine PET in detecting neuropathologically confirmed recurrent brain tumor after radiation therapy. *Ann. Nucl. Med.* **32**, 132-141 (2018).

15. Terakawa, Y. *et al.* Diagnostic accuracy of 11C-methionine PET for differentiation of recurrent brain tumors from radiation necrosis after radiotherapy. *J. Nucl. Med.* **49**, 694-699 (2008).

16. Galldiks, N. *et al.* Use of 11C-methionine PET to monitor the effects of temozolomide chemotherapy in malignant gliomas. *Eur. J. Nucl. Med. Mol. Imaging.* **33**, 516-524 (2006).

17. Glaudemans, A.W. *et al.* Value of 11C-methionine PET in imaging brain tumours and metastases. *Eur. J. Nucl. Med. Mol. Imaging.* **40**, 615-635 (2013).

18. Hotta, M., Minamimoto, R., Miwa, K. 11C-methionine-PET for differentiating recurrent brain tumor from radiation necrosis: radiomics approach with random forest classifier. *Sci Rep.* **9**, 15666; 10.1038/s41598-019-52279-2 (2019).

19. Iwadate, Y., Shinozaki, N., Matsutani, T., Uchino, Y., Saeki, N. Molecular imaging of 1p/19q deletion in oligodendroglial tumours with 11C-methionine positron emission tomography. *J. Neurol. Neurosurg. Psychiatry.* **87**, 1016-1021 (2016).

20. Ishiwata, K., Ido, T., Abe, Y., Matsuzawa, T., Iwata, R. Tumor uptake studies of S-adenosyl-L-[methyl-11C]methionine and L-[methyl-11C]methionine. *Int. J. Rad. Appl. Instrum. B.* **15**, 123-126 (1988).

21. Akamatsu, G. *et al.* Influence of statistical fluctuation on reproducibility and accuracy of SUVmax and SUVpeak: a phantom study. *J. Nucl. Med. Technol.* **43**, 222-226 (2015).

22. Youden. W.J. Index for rating diagnostic tests. *Cancer.* **3**, 32-35 (1950).

23. Herholz, K. *et al.* 11C-methionine PET for differential diagnosis of low-grade gliomas. *Neurology.* **50**, 1316-1322 (1998).

24. Renard, D. *et al.* 18 F-FDOPA-PET in pseudotumoral brain lesions. *J. Neurol.* **268**, 1266-1275 (2021).

25. Okubo, S., Zhen, H.N., Kawai, N., Nishiyama, Y., Haba, R., Tamiya, T. Correlation of L-methyl-11C-methionine (MET) uptake with L-type amino acid transporter 1 in human gliomas. *J. Neurooncol.* **99**, 217-225 (2010).

26. Pasternak, K.A. *et al*. Evaluation of 311 contemporary cases of stereotactic biopsies in patients with neoplastic and non-neoplastic lesions-diagnostic yield and management of non-diagnostic cases. *Neurosurg. Rev.* 10.1007/s10143-020-01394-0 (2020).

27. Jagannathan, J. *et al.* Clinical and pathological characteristics of brain metastasis resected after failed radiosurgery. *Neurosurgery.* **66**, 208-217 (2010).

28. Nakajima, R., Kimura, K., Abe, K., Sakai, S. (11)C-methionine PET/CT findings in benign brain disease. *Jpn. J. Radiol.* **35**, 279-288 (2017).

29. Lapa, C. *et al.* Comparison of 11C-choline and 11C-methionine PET/CT in multiple myeloma. *Clin. Nucl. Med.* **44**, 620-624 (2019).

30. Lapa, C. *et al.* 11C-Methionine-PET in multiple myeloma: a combined study from two different institutions. *Theranostics.* **7**, 2956-2964 (2017).

31. Kircher, S. *et al.* Hexokinase-2 Expression in 11C-methionine-positive, 18F-FDG-negative multiple myeloma. *J. Nucl. Med.* **60**, 348-352 (2019).

32. Zaharchuk, G., Davidzon, G. Artificial intelligence for optimization and interpretation of PET/CT and PET/MR images. *Semin, Nucl, Med.* **51**, 134-142 (2021).

33. Seifert, R., Weber, M., Kocakavuk, E., Rischpler, C., Kersting, D. Artificial intelligence and machine learning in nuclear medicine: future perspective. *Semin. Nucl. Med.* **51**, 170-177 (2021).

34. Liu, X., Chen, K., Wu, T., Weidman, D., Lure, F., Li, J. Use of multimodality imaging and artificial intelligence for diagnosis and prognosis of early stages of Alzheimer's disease. *Transl. Res.* **194**, 56-67 (2018).

35. Tanno, R. *et al.* Uncertainty modelling in deep learning for safer neuroimage enhancement: Demonstration in diffusion MRI. *Neuroimage.* **225**, 117366; 10.1016/j.neuroimage.2020.117366 (2021).

36. D'Souza, M.M. *et al.* Metabolic assessment of intracranial tuberculomas using 11C-methionine and 18F-FDG PET/CT. *Nucl. Med. Commun.* **33**, 408-414 (2012).

37. Ng, D., Jacobs, M., Mantil, J. Combined C-11 methionine and F-18 FDG PET imaging in a case of neurosarcoidosis. *Clin. Nucl. Med.* **31**, 373-375 (2006).

Tables

TABLE 1 Comparison of radiological diagnoses on ^{11}C-METPET with definitive diagnoses

TABLE 1

Radiological diagnosis of ^{11}C-MET-PET	Number of final diagnosis			Concordance rate (%)
	Brain tumors	Non-neoplastic lesions	Undetermined	
Brain tumors	70	3	6	88.6
Non-neoplastic lesions	5	19	4	67.9
Equivocal	3	1	2	
Total	78	23	12	

TABLE 2

	Mean ± SD for								
	Brain tumors (n = 78)					Non-neoplastic lesions (n = 23)			
Index	High grade CNS tumor (n = 31)	Low grade CNS tumor (n = 37)	Glioma, not otherwise specified (n = 5)	Lymphoma (n = 3)	Metastatic brain tumor (n = 2)	Neurovascular disease (n = 10)	Dysplasia (n = 5)	Encephalopathy (n = 4)	Inflammatory disease (n = 4)
SUVmean	4.64 ± 2.68	2.92 ± 1.32	2.78 ± 2.49	4.4 ± 1.97	7.07 ± 1.8	1.27 ± 0.67	1.65 ± 1.02	1.59 ± 0.76	2.95 ± 2.14
SUVpeak	4.33 ± 2.46	2.91 ± 1.31	2.89 ± 2.48	3.78 ± 1.44	7.17 ± 1.94	1.41 ± 0.49	1.72 ± 0.98	1.61 ± 0.54	2.74 ± 1.73
SUVmax	6.51 ± 3.5	4.08 ± 1.87	3.81 ± 3.32	6.55 ± 2.93	9.94 ± 3.18	1.88 ± 0.95	2.42 ± 1.4	2.39 ± 1.32	4.05 ± 2.87
Lmax/Nmean	4.85 ± 2.47	2.93 ± 1.22	2.39 ± 1.54	5.27 ± 3.77	6.11 ± 1.9	1.34 ± 0.62	1.68 ± 0.96	1.66 ± 0.25	2.76 ± 1.73
Lmax/Nmax	3.84 ± 1.89	2.36 ± 0.94	1.99 ± 1.24	4.51 ± 3.26	5.04 ± 1.43	1.1 ± 0.51	1.4 ± 0.79	1.34 ± 0.19	2.14 ± 1.38

CNS = central nervous system; SUV = standardized uptake value; L/N = lesion-to-normal tissue ratio; Data are mean ± SD.

TABLE 2 Quantitative analysis for the definitive diagnosis of intracranial lesions

TABLE 3

Diagnostic value	cutoff value	% Sensitivity	% Specificity	% PPV	% NPV
Lmax/Nmax	> 2.01	70.5	91.3	96.5	47.4
Lmax/Nmean	> 2.23	75.6	82.6	93.7	50

PPV = positive predictive value; NPV = negative predictive value

TABLE 3 Optimal cut-off values and their diagnostic accuracy for intracranial tumors

Figures

FIGURE 1

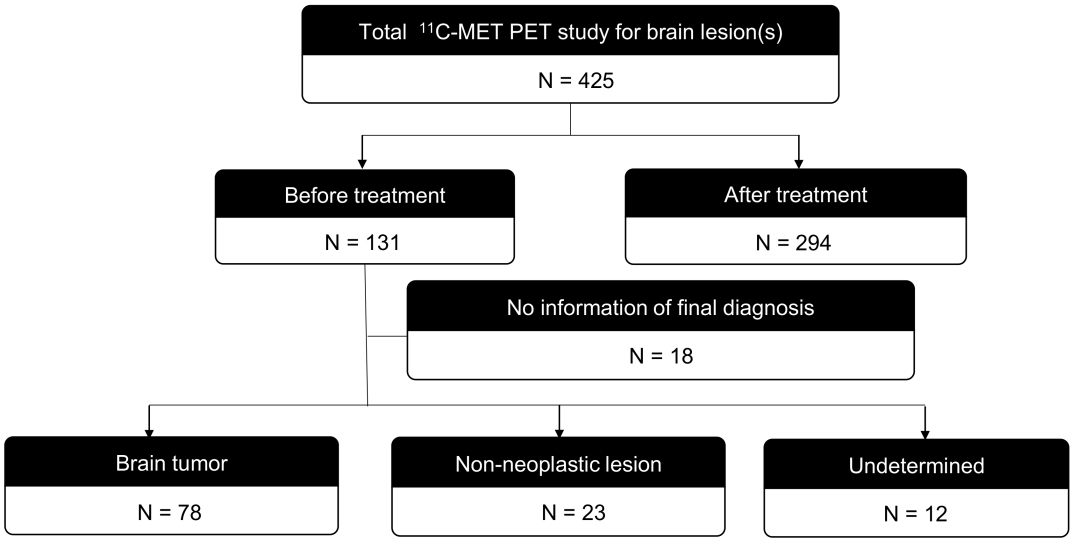

Figure 1

Flow chart showing the process for patient-based lesion validation in this study of pre-treatment brain lesions. In total, 78 patients had validated brain tumors and 23 patients had non-neoplastic lesions. The final diagnosis remained undetermined in 12 patients.

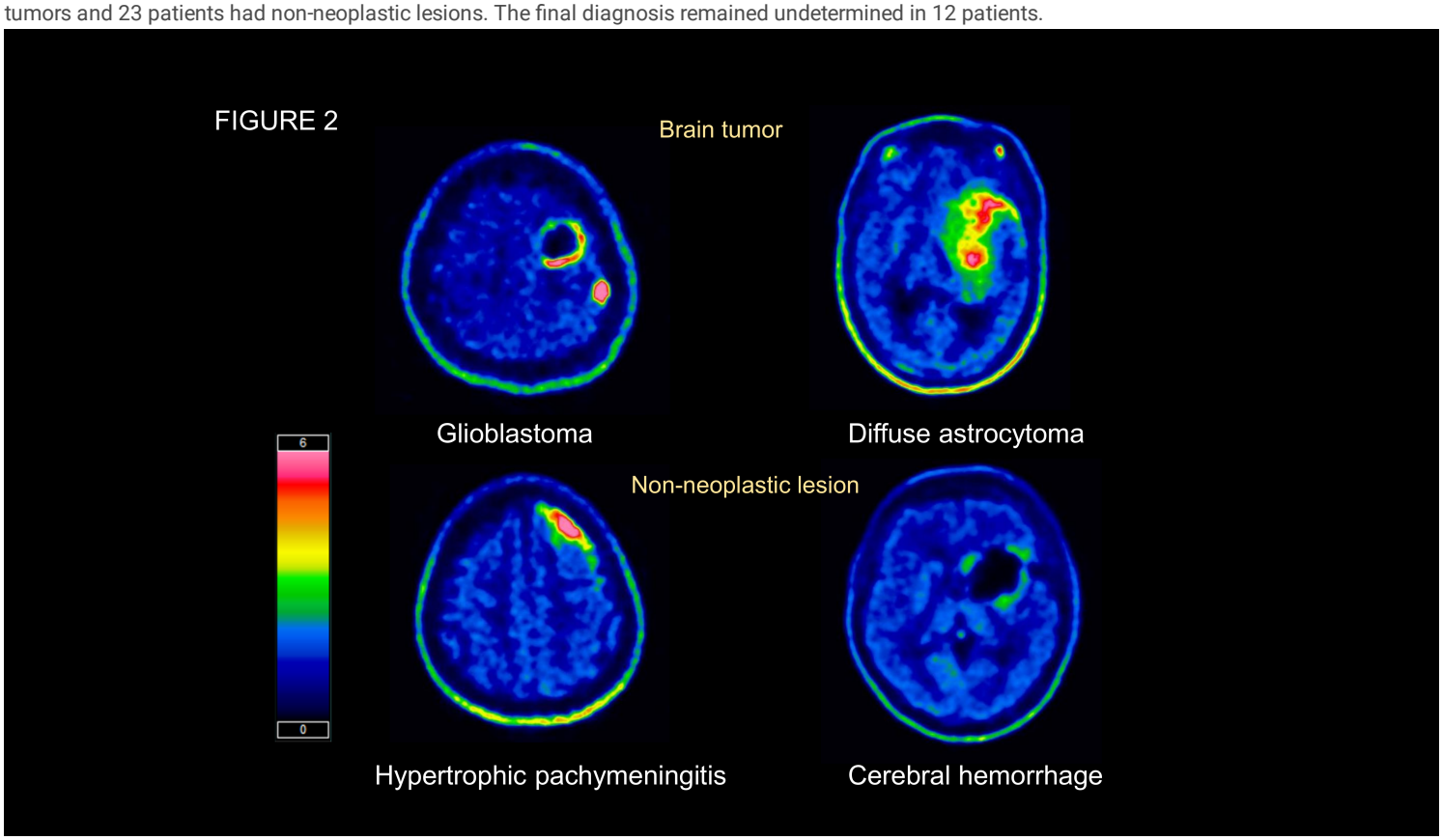

Figure 2

11C-METPET images from typical subjects with glioblastoma, diffuse astrocytoma, hypertrophic pachymeningitis, and cerebral hemorrhage.

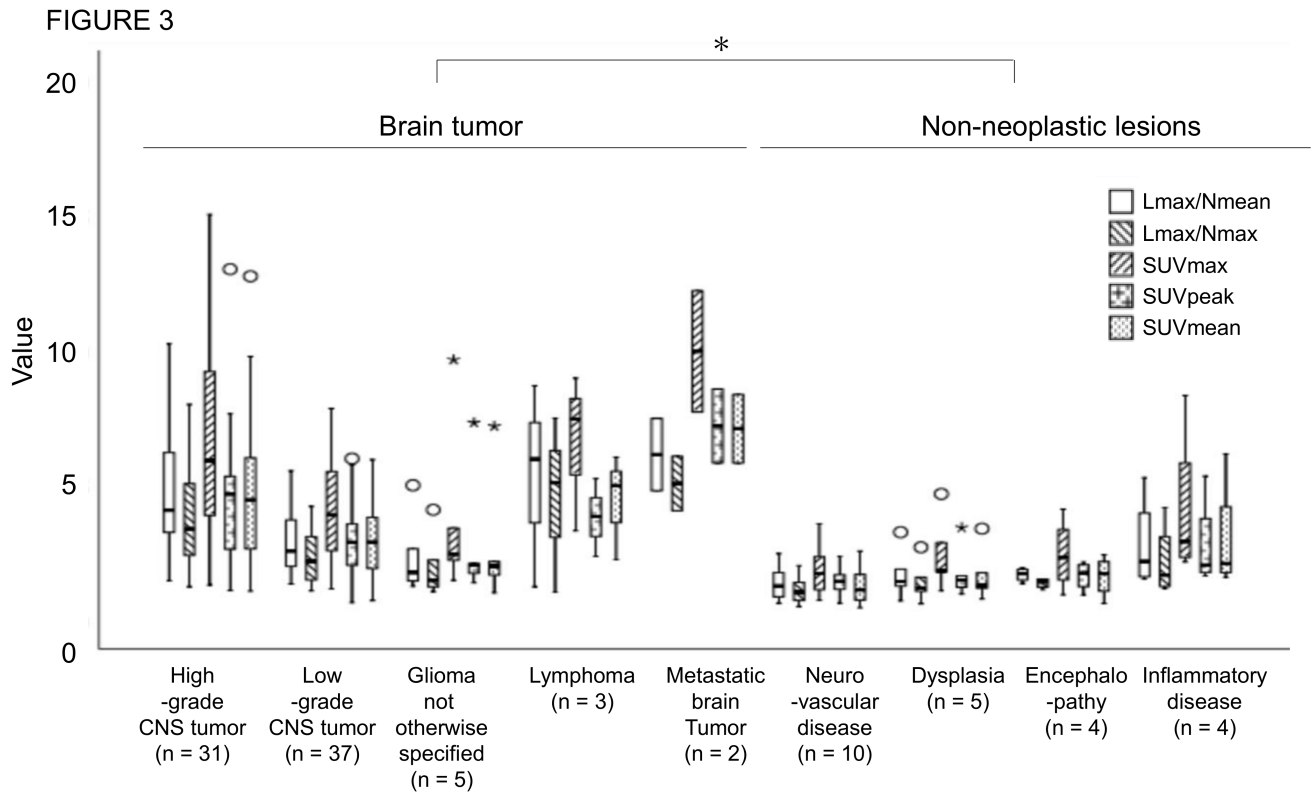

Figure 3

Box-and-whisker plots of each 11C-METPET parameter for brain tumors and non-neoplastic lesions. Asterisks (*) indicate significant differences in all parameters between brain tumors and non-neoplastic lesions ($p < 0.001$). The bottom and top of the boxes indicate the 25th and 75th percentiles, respectively, and the lines inside the boxes indicate the 50th percentile. Circles (○) indicate outliers and stars (☆) indicate extreme outliers that are more than three times the height of the box.

FIGURE 4

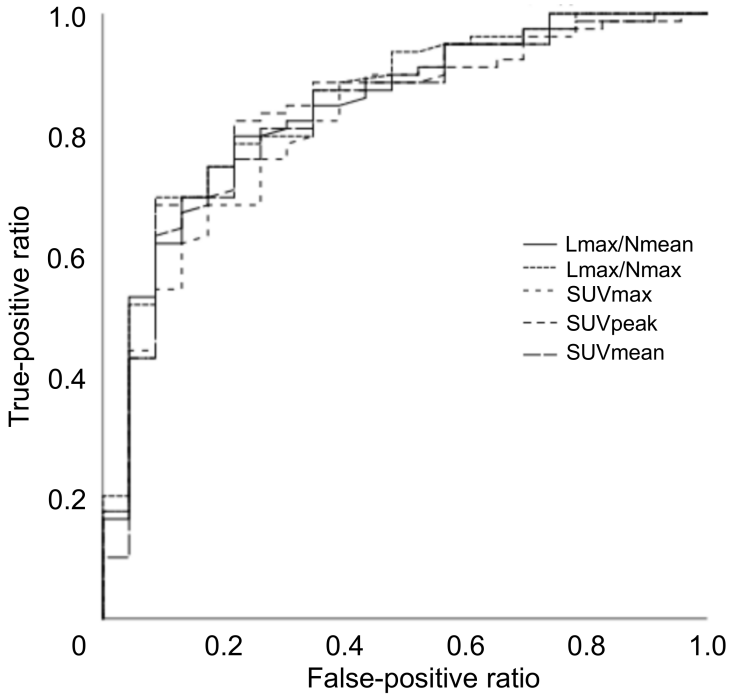

Figure 4

Receiver operating characteristics curves for the differentiation between brain tumors and non-neoplastic lesions by methionine uptake parameters including Lmax/Nmean, Lmax/Nmax, SUVmax, SUVpeak, and SUVmean. The areas under the curve were 0.843 for Lmax/Nmean, 0.853 for Lmax/Nmax, 0.821 for SUVmax, 0.837 for SUVpeak, and 0.829 for SUVmean.